

Stable all-optical limiting in nonlinear periodic structures. I. Analysis

Dmitry Pelinovsky

Department of Mathematics, McMaster University, Hamilton, Ontario, Canada, L8S 4K1

Jason Sears, Lukasz Brzozowski, and Edward H. Sargent

Department of Electrical and Computer Engineering, University of Toronto, Toronto, Ontario, Canada, M5S 1A4

Received September 6, 2000; revised manuscript received March 2, 2001

We consider propagation of coherent light through a nonlinear periodic optical structure consisting of two alternating layers with different linear and nonlinear refractive indices. A coupled-mode system is derived from the Maxwell equations and analyzed for the stationary-transmission regimes and linear time-dependent dynamics. We find the domain for existence of true all-optical limiting when the input-output transmission characteristic is monotonic and clamped below a limiting value for output intensity. True all-optical limiting can be managed by compensating the Kerr nonlinearities in the alternating layers, when the net-average nonlinearity is much smaller than the nonlinearity variance. The periodic optical structures can be used as uniform switches between lower-transmissive and higher-transmissive states if the structures are sufficiently long and out-of-phase, i.e., when the linear grating compensates the nonlinearity variations at each optical layer. We prove analytically that true all-optical limiting for zero net-average nonlinearity is asymptotically stable in time-dependent dynamics. We also show that weakly unbalanced out-of-phase gratings with small net-average nonlinearity exhibit local multistability, whereas strongly unbalanced gratings with large net-average nonlinearity display global multistability. © 2002 Optical Society of America

OCIS codes: 230.4320, 190.1450, 190.4360.

1. INTRODUCTION

Fiber-optic communications networks operate at information rates unachievable by electronic signal generation alone. Optical components are used to multiplex many independently modulated wavelength channels onto a single physical medium. In addition, all-optical multiplexing and demultiplexing have been demonstrated purely in the time domain: in these systems the signaling rate on a single channel vastly exceeds rates possible through direct electronic coding.

In today's fiber-optic networks the use of all-optical processing (the regeneration and routing of information-bearing optical signals) may yield a dramatic savings in power and cost. In future optical time-division multiplexed systems it will be the only option for the management of bursts of data. Optical signal-processing elements will exploit the speed and parallelism inherent to optics and accommodate future bandwidth growth.¹⁻³

Passive optical limiters represent one important family of optical signal-processing elements. Existing mechanisms include total internal reflection,⁴ two-photon absorption and photorefractive beam fanning,⁴ self-focusing,^{5,6} reverse saturable absorption,⁷ and soliton trapping in nonlinear optical fiber.⁸⁻¹⁰ In contrast with applications in information storage, optical signal-processing operations require devices that are uniformly stable for all pertinent incident intensities. Passive optical limiters do support under different technological constraints a uniformly stable operating regime, which we term here true all-optical limiting.

We have recently proposed and elaborated¹¹ new passive optical limiters based on nonlinear reflection of light instead of absorption. We have shown that, in combination, these devices can provide a full set of logic functions. The nonlinear reflection-based limiters are composed of multilayer structures in which the linear and nonlinear refractive indices vary periodically. We have shown that, if fabricated with available nonlinear materials, these devices may exhibit a dramatically reduced intensity threshold for the onset of true all-optical limiting. They may be made strongly wavelength selective in order to act on a single channel in a multiwavelength system.

Periodically nonlinear optical materials generally exhibit the widely studied phenomena of bistability and multistability. As a result, these materials do not lead to memoryless (hysteresis-free) operation.¹²⁻¹⁶ They do not exhibit saturation of the transmitted intensity to a limiting value and may undergo chaotic behavior.¹⁷ In contrast, in real-time signal processing, bit-level signal-regeneration operations such as edge sharpening, retiming, and signal-to-noise enhancement should be independent of the past state of the channel.

The center frequency of the stopband must be largely independent of intensity in order to obtain stability in a nonlinear periodic device. In our recent work^{11,18} we considered refraction of incoherent light in optical gratings of alternating layers with Kerr coefficients of opposite signs. We have shown that multistability disappears if the Kerr nonlinearities are compensated with zero or a small average over the many-layered structure but possess high lo-

cal nonlinearity inside each individual layer. We term this method of compensating Kerr nonlinearities nonlinearity management of the refractive optical gratings.

Nonlinearity management is widely employed in the fabrication of structures based on second-harmonic generation to achieve quasi phase matching of the nonlinear interactions.^{19–21} However, such systems are used for sending short-pulse nonresonant signals over a long propagation scale. In this aspect our work is distinct because we consider optical devices based on the Bragg resonance between the wavelength of light and the period of the spatially varying nonlinearity. It is these short-scale resonant devices that are of use in memory applications of bistable and multistable regimes when nonlinearity management is neglected.^{12,22}

We have recently analyzed and quantified the response of a nonlinear periodic optical structure illuminated by coherent light waves. In particular, we focus on the conditions under which the nonlinearity-managed grating works in the operating regime of true all-optical limiting. In the present paper we develop, for the first time to our knowledge, a complete analytical theory of true all-optical limiting in the nonlinear optical gratings.

Starting from the Maxwell equations, we derive in Section 2 the coupled-mode equations for coherent light waves propagating through the nonlinear distributed-feedback structure. The domain for existence of a true all-optical limiting regime is found in Section 3. A linear time-evolution analysis is developed in Section 4 wherein we present the analytical proof of stability of the true all-optical limiting.

2. THEORETICAL MODEL

We consider the periodic nonlinear structure illustrated in Fig. 1. The finite-length optical device consists of N alternating layers with different linear refractive indices and different Kerr nonlinearities. In the well-known averaged approximation²³ the refractive index of an optical material is $n(z, |E|^2) = n_0(z) + n_2(z)|E|^2 + O(|E|^4)$, where $n_0(z)$ and $n_2(z)$ are linear and Kerr nonlinear indices, respectively, and z is the direction along the structure. The indices $n_0(z)$ and $n_2(z)$ are constant within each layer as in Fig. 1.

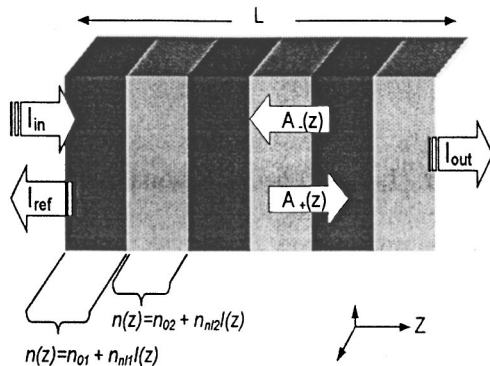


Fig. 1. Periodic nonlinear structure consisting of alternating layers with different linear refractive indices and different Kerr nonlinearities.

Depending on the material and the optical wavelength, the refractive index may increase or decrease with the intensity, i.e., the component $n_2(z)$ may be either positive or negative. We show in Sections 3 and 4 that the periodic nonlinear grating provides true all-optical limiting if the net-average nonlinear index $n_{nl} = \langle n_2(z) \rangle$ is much smaller than the variation in the nonlinear index between individual layers $(\Delta n_{nl})^2 = \langle [n_2(z) - n_{nl}]^2 \rangle$. In order to prove this main result we derive here a set of coupled-mode equations for coherent wave propagation in the periodic optical structure.

We study the nonstationary Maxwell equations averaged across a transverse cross section (x, y) . We assume linear polarization of coherent light and no two-photon absorption effects:

$$\frac{\partial^2 \mathbf{E}}{\partial z^2} - \frac{n^2(z, |E|^2)}{c^2} \frac{\partial^2 \mathbf{E}}{\partial t^2} = 0, \quad (1)$$

where $E(z, t)$ is a scalar electric field and $c = (\epsilon_0 \mu_0)^{-1/2}$ is the speed of light. Light whose wavelength lies within the linear forbidden band is incident upon the medium. The two counterpropagating waves are then strongly coupled, and the intensity-dependent refraction of the optical material supports resulting transmission of light through the periodic structure (Fig. 1). For analysis the Maxwell equations can be simplified when the variations of the refractive index due to nonlinearity and linear grating are much smaller than the average index $n_{ln} = \langle n_0(z) \rangle$. If the small spatial variations of indices $n_0(z)$ and $n_2(z)$ have the same spatial symmetry centered at $z = 0$, then $n(z, |E|^2)$ can be expanded into the Fourier series,

$$n(z, |E|^2) = n_{ln} + 2n_{0k} \cos kz + n_{nl}|E|^2 + 2n_{2k}|E|^2 \cos kz, \quad (2)$$

where $|n_{0k}|$, $|n_{nl}||E|^2$, $|n_{2k}||E|^2 \ll |n_{ln}|$, $k = 2\pi/\Lambda$ is the wave number inside the material, and Λ is the period of the structure so that the total length is $l = N\Lambda$. The Fourier series for $E(z, t)$ in the model (1) and (2) is then given in the same approximation as

$$E(z, t) = A_+(z, t) \exp[i(k_0 z - \omega_0 t)] + A_-(z, t) \exp[-i(k_0 z + \omega_0 t)] + \text{higher-order terms}, \quad (3)$$

where $\omega_0 = ck_0/|n_{ln}|$ is the light frequency and $k_0 = 2\pi|n_{ln}|/\lambda$ is the light wave number. The resonance in the first gap occurs for $k = 2k_0$, i.e., when the optical wavelength λ matches the period of the structure, $\lambda = 2|n_{ln}|\Lambda$. Near the resonance the amplitudes $A_{\pm} = A_{\pm}(z, t)$ satisfy the coupled-mode system easily derived from Eqs. (1)–(3) in the assumption $|\partial A_{\pm}/\partial z|$, $|\partial A_{\pm}/\partial t| \ll |A_{\pm}|$,

$$i \left(\frac{\partial A_+}{\partial Z} + \frac{\partial A_+}{\partial T} \right) + n_{0k} A_- + n_{nl} (|A_+|^2 + 2|A_-|^2) A_+ + n_{2k} [(2|A_+|^2 + |A_-|^2) A_- + A_+^2 \bar{A}_-] = 0, \quad (4)$$

$$-i\left(\frac{\partial A_-}{\partial Z} - \frac{\partial A_-}{\partial T}\right) + n_{0k}A_+ + n_{nl}(2|A_+|^2 + |A_-|^2)A_- \\ + n_{2k}[(|A_+|^2 + 2|A_-|^2)A_+ + A_-^2\bar{A}_+] = 0, \quad (5)$$

where $Z = \omega_0 z/c$ and $T = \omega_0 t/|n_{ln}|$ are the normalized spatial coordinate and time, respectively. For the two-layer structure shown in Fig. 1 the Fourier coefficients of expansion (2) can be evaluated from the constant linear and nonlinear indices in each layer,

$$n_{ln} = \frac{n_{01} + n_{02}}{2}, \quad n_{nl} = \frac{n_{nl1} + n_{nl2}}{2}, \\ n_{0k} = \frac{n_{01} - n_{02}}{\pi}, \quad n_{2k} = \frac{n_{nl1} - n_{nl2}}{\pi}. \quad (6)$$

Here and in the rest of the paper, we use normalized intensity in units reciprocal to the units of n_{nl} .

Special cases of the coupled system (4) and (5) have been already studied for the phenomena of optical bistability and gap solutions.^{12,17} For $n_{2k} = 0$ (no management of Kerr nonlinearities) this system is readily derived for linear Bragg gratings.²² For $n_{2k} \neq 0$ but $A_{\pm} = A_{\pm}(z)$ (stationary regime) the same model can be identified from Eqs. (10a) and 10(b) of He and Cada¹⁶ who studied semiconductor structures and GaAs-AlAs superlattices.

In the present work we are particularly interested in the regime, when $n_{nl} = 0$ but $n_{2k} \neq 0$. In this case, coupled-mode theory prescribes a new phenomenon: true all-optical limiting. Since many results are available for other cases but the regime of true all-optical limiting was overlooked in previous works, we undertake a special consideration of this regime. In this paper we analyze two major problems: (i) domain for existence of the stationary limiting regime and (ii) the linear stability problem for the limiting transmission. We prove that the true all-optical limiting is indeed marginally stable within the model (4) and (5) for $|n_{nl}| \ll |n_{2k}|$. The linear index mismatch n_{0k} does not change this conclusion for large intensities of the incident wave, but it does modify the value for limiting intensity and also the shape of the input-output transmission characteristic. A sufficiently large mismatch n_{0k} or more layers N for out-of-phase gratings lead to local multistability for lower and higher intensities. We determine the threshold between locally multistable and uniformly stable regimes as well as the threshold between true all-optical limiting and global multistability of the nonlinear grating.

3. DOMAIN FOR EXISTENCE OF THE LIMITING REGIME

Here we consider the stationary regime for the transmission of coherent light through the periodic nonlinear structure; i.e., we set $\partial A_{\pm}/\partial T = 0$. The standard scattering problem is imposed for the amplitudes $A_{\pm}(Z)$ by the boundary conditions at the left and right ends of the structure, $Z = 0$ and $Z = L = \omega_0 l/c$ (see Fig. 1), where

$$|A_+(0)|^2 = I_{in}, \quad |A_-(0)|^2 = I_{ref}, \\ |A_+(L)|^2 = I_{out}, \quad |A_-(L)|^2 = 0. \quad (7)$$

Here I_{in} , I_{ref} , and I_{out} are intensities of incident, reflected, and transmitted waves. The stationary equations (4) and (5) preserve the intensity flow through the structure,

$$|A_+(Z)|^2 - |A_-(Z)|^2 = I_{in} - I_{ref} = I_{out}. \quad (8)$$

The stationary equations can be written in the Hamiltonian form,

$$\frac{\partial A_{\pm}}{\partial Z} = \pm i \frac{\partial H}{\partial \bar{A}_{\pm}}, \quad (9)$$

where the conserved (real-valued) Hamiltonian is

$$H = [n_{0k} + n_{2k}(|A_+|^2 + |A_-|^2)](\bar{A}_+A_- + A_+\bar{A}_-) \\ + \frac{1}{2}n_{nl}(|A_+|^4 + 4|A_+|^2|A_-|^2 + |A_-|^4). \quad (10)$$

Since two conserved quantities (8) and (10) exist for two complex equations for $A_+(Z)$ and $A_-(Z)$, the system (9) is integrable. We use flow equation (8) to parameterize the solution in the polar form,

$$A_+(Z) = \sqrt{I_{out} + Q} \exp[i(\Phi - \Psi)], \\ A_-(Z) = \sqrt{Q} \exp(i\Phi) \quad (11)$$

where $Q(Z)$ and $\Phi(Z)$ are the intensity and the complex phase of the reflected wave and $\Psi(Z)$ is the phase mismatch between the incident and reflected waves. The system (4) and (5) can be reduced in the form (11) to the coupled system for $Q(Z)$ and $\Psi(Z)$,

$$\frac{dQ}{dZ} = -2\sqrt{Q(I_{out} + Q)} \sin \Psi [n_{0k} + n_{2k}(I_{out} + 2Q)], \quad (12)$$

$$\frac{d\Psi}{dZ} = -3n_{nl}(I_{out} + 2Q) - \frac{\cos \Psi}{\sqrt{Q(I_{out} + Q)}} \\ \times [n_{0k}(I_{out} + 2Q) + n_{2k}(I_{out}^2 + 8I_{out}Q + 8Q^2)]. \quad (13)$$

It follows from Eqs. (10) and (11) that, in the coupled system, the quantity

$$H = 2\sqrt{Q(I_{out} + Q)} \cos \Psi [n_{0k} + n_{2k}(I_{out} + 2Q)] \\ + 3n_{nl}Q(I_{out} + Q) + \frac{1}{2}n_{nl}I_{out}^2 \quad (14)$$

is conserved. The boundary conditions (7) are satisfied for $H = \frac{1}{2}n_{nl}I_{out}^2$, when $Q(Z)$ and $\Psi(Z)$ are connected by the relation

$$\cos \Psi = \frac{-3n_{nl}\sqrt{Q(I_{out} + Q)}}{2[n_{0k} + n_{2k}(I_{out} + 2Q)]}. \quad (15)$$

The coupled system (12) and (13) can be reduced with the help of Eq. (15) to a single equation either for $Q(Z)$ or for $\Psi(Z)$ [see Eq. (28) below]. However, this reduction depends on the parameters n_{nl} , n_{0k} , n_{2k} , and I_{out} of the model. Here we consider two different cases: (i) $n_{nl} = 0$ and (ii) $n_{nl} \neq 0$. In the first case we find explicit elementary solutions of the system that enable us to classify all stationary-transmission regimes for the periodic structure with balanced (zero-average) nonlinearity management. In the other case the exact solutions are given in terms of implicit elliptic integrals. Instead of full analysis of the case (ii) we study only new features in the stationary transmission through the periodic structure compared with the case (i).

A. Balanced (Zero-Average) Nonlinearity Management: $n_{nl}=0$

When the periodic structure consists of alternating layers with zero net-average Kerr nonlinearity, the coupled-mode equations (12) and (13) become simple and analytically tractable. Since true all-optical limiting is best achieved and performed in this regime, we develop a complete analysis of the system (12) and (13) in this case.

First, we need to satisfy the boundary condition $Q(L) = 0$ and $Q(Z) \geq 0$ for the intensity of the reflected wave at the right end of the structure [i.e., the slope of $Q(Z)$ is negative near $Z \approx L$]. Matching Eqs. (12) and (15), we conclude that the phase factor $\Psi(Z)$ is constant in the case $n_{nl} = 0$ and has the following boundary conditions:

$$\Psi(Z) = \frac{\pi}{2} \quad \text{for } n_{0k} + n_{2k}I_{out} \geq 0, \quad (16)$$

$$\Psi(Z) = -\frac{\pi}{2} \quad \text{for } n_{0k} + n_{2k}I_{out} < 0. \quad (17)$$

We may assume without loss of generality that the first layer is focusing and the second one is defocusing so that $n_{2k} > 0$ [see Eq. (6)]. Under this convenient agreement we interpret the negative values of n_{0k} as out-of-phase matching between linear and Kerr nonlinear refractive indices and the positive values of n_{0k} as in-phase matching of the indices.

We consider first the case when $|n_{0k}| \leq n_{2k}I_{out}$. Direct integration of Eq. (12) for $\Psi(Z) = \pi/2$ produces the explicit solutions

$$Q(Z) = \frac{I_{out}(n_{0k} + n_{2k}I_{out})\sin^2 \theta}{n_{2k}I_{out} \cos 2\theta - n_{0k}}, \quad (18)$$

where $\theta = \sqrt{n_{2k}^2 I_{out}^2 - n_{0k}^2}(L - Z)$. It is clear that the solution $Q(Z)$ is monotonically decreasing between $Z = 0$ and $Z = L$ and is defined for $I_{out} \leq I_{lim}$, where I_{lim} solves the transcendent equation

$$-1 \leq \cos(2\sqrt{n_{2k}^2 I_{lim}^2 - n_{0k}^2}L) = \frac{n_{0k}}{n_{2k}I_{lim}} \leq 1. \quad (19)$$

Parameter I_{lim} represents the limiting value for the transmitted intensity that characterizes the output of the nonlinear periodic structure. Typical transmission (input-output) curves $I_{out} = I_{out}(I_{in})$ are displayed in Fig. 2 for $n_{2k} = 1$ and three different values of n_{0k} . The transmitted intensity I_{out} is a one-to-one function of the incident intensity I_{in} and is bounded by its limiting value I_{lim} (shown in Fig. 2 by horizontal lines).

Using Eq. (19), we can readily consider the limit when the linear grating is weak compared with the nonlinearity management, i.e., $|n_{0k}| \ll n_{2k}I_{lim}$. In this case the limiting intensity can be approximated explicitly as

$$I_{lim} = \frac{\pi}{4n_{2k}L} \left[1 - \frac{8n_{0k}L}{\pi^2} + O(n_{0k})^2 \right]. \quad (20)$$

It is clear from Fig. 2 that the limiting regime with $I_{lim} \approx 0.01$ and $n_{2k} = 1$ is supported by a nonlinear change in the refractive index higher than 1%. This is an extremely high estimate for Kerr nonlinearities, and it cannot be achieved in any realistic optical materials. However, as follows from Eq. (20), the limiting intensity is inversely proportional to the length of optical devices. Using longer devices would require lower index changes that are more realistic. Long multiperiodic nonlinear structures can be fabricated from colloidal crystals; see, e.g., Ref. 24.

It also follows from Eq. (20) that the limiting value becomes smaller for the in-phase gratings, when $n_{0k} > 0$, and it grows for the out-of-phase gratings, when $n_{0k} < 0$. Therefore no matter how large the mismatch between linear and nonlinear refractive indices is built, true all-optical limiting is still achieved for out-of-phase gratings with sufficiently large input (and output) intensities. We express this property by the estimate on the limiting intensity,

$$I_{lim} \geq \frac{|n_{0k}|}{n_{2k}} \quad \text{for } n_{0k} < 0, \quad n_{nl} = 0. \quad (21)$$

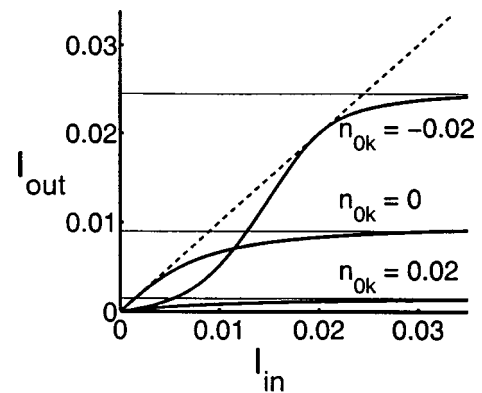


Fig. 2. Balanced nonlinearity management with a linear grating, where $n_{nl} = 0$, $n_{2k} = 1$. Horizontal lines show the limiting intensity I_{lim} , and the dashed line displays the regime of complete transparency: $I_{out} = I_{in}$. An out-of-phase ($n_{0k} = -0.02$) grating increases I_{lim} , whereas an in-phase grating ($n_{0k} = 0.02$) decreases it.

The other (in-phase) gratings always support true all-optical limiting with no constraints on the value for the limiting intensity I_{lim} . This value reduces with larger mismatch $n_{0k} > 0$.

We consider now the case when $|n_{0k}| > n_{2k}I_{\text{out}}$. The exact solution (18) can be generalized to the form

$$Q(Z) = \frac{I_{\text{out}}(n_{0k} + n_{2k}I_{\text{out}})\sinh^2 \phi}{n_{0k} - n_{2k}I_{\text{out}} \cosh 2\phi}, \quad (22)$$

where $\phi = -i\theta = \sqrt{n_{0k}^2 - n_{2k}^2 I_{\text{out}}^2}(L - Z)$. It may be verified that this expression does indeed solve Eq. (12) for $\Psi(Z) = \pi/2$ when $n_{0k} > 0$ and for $\Psi(Z) = -\pi/2$ when $n_{0k} < 0$. The behavior of the wave profile $Q(Z)$ across the structure is now different depending on the sign of n_{0k} .

In the case when $n_{0k} > 0$ (in-phase gratings), solution (22) is nonsingular for $I_{\text{out}} \leq \min(I_{\text{lim}}, n_{0k}/n_{2k})$. If $I_{\text{lim}} > n_{0k}/n_{2k}$, the transmission curve $I_{\text{out}} = I_{\text{out}}(I_{\text{in}})$ consists of two pieces that are described by the solutions (18) for $n_{0k}/n_{2k} < I_{\text{out}} < I_{\text{lim}}$ and (22) for $I_{\text{out}} < n_{0k}/n_{2k}$. These two solutions match in the limit $I_{\text{out}} \rightarrow n_{0k}/n_{2k}$, where the formulas (18) and (22) produce a unique result,

$$Q(Z) = \frac{4I_{\text{out}}n_{0k}^2(L - Z)^2}{1 - 4n_{0k}^2(L - Z)^2} \quad \text{as } I_{\text{out}} \rightarrow \frac{n_{0k}}{n_{2k}} > 0. \quad (23)$$

This expression is nonsingular for $n_{0k} \leq 1/(2L)$. Otherwise, i.e., when $n_{0k} > 1/(2L)$, the whole input–output curve $I_{\text{out}}(I_{\text{in}})$ lies below the value $I_{\text{out}} = n_{0k}/n_{2k}$ and is described solely by Eq. (22). In the latter case shown in Fig. 2 for $n_{0k} = 0.02$, the limiting intensity satisfies the estimate $I_{\text{lim}} \leq n_{0k}/n_{2k}$ and can be found by solving the transcendental equation

$$\cosh(2\sqrt{n_{0k}^2 - n_{2k}^2 I_{\text{lim}}^2}L) = \frac{n_{0k}}{n_{2k}I_{\text{lim}}} > 1. \quad (24)$$

In contrast, in the case $n_{0k} < 0$ (out-of-phase gratings), solution (22) is never singular and exists for the whole domain $0 \leq I_{\text{out}} < |n_{0k}|/n_{2k}$. The transmission curve $I_{\text{out}}(I_{\text{in}})$ shown in Fig. 2 for $n_{0k} = -0.02$ touches the straight line $I_{\text{in}} = I_{\text{out}}$ (dotted diagonal line) at the value $I_{\text{out}} = |n_{0k}|/n_{2k}$, where the solution is trivial: $Q(Z) = 0$. It implies that the out-of-phase periodic nonlinear structure is completely transparent for $I_{\text{in}} = |n_{0k}|/n_{2k}$, i.e., the nonlinear index variations are completely compensated by the out-of-phase linear grating. The value $I_{\text{in}} = I_{\text{out}} = |n_{0k}|/n_{2k}$ is a meeting point that matches two pieces of the curve $I_{\text{out}}(I_{\text{in}})$ that are expressed by the explicit solutions (18) and (22). Near the meeting point, we find from Eqs. (18) and (22) an asymptotic solution for $Q(Z)$ in the limit $n_{0k} + n_{2k}I_{\text{out}} \rightarrow 0$,

$$Q(Z) = I_{\text{out}}(n_{0k} + n_{2k}I_{\text{out}})^2(L - Z)^2. \quad (25)$$

This asymptotic solution implies that the curve $I_{\text{out}}(I_{\text{in}})$ is concave-down near $I_{\text{out}} = |n_{0k}|/n_{2k}$ so that there is an inflection point in the interval $0 < I_{\text{out}} < |n_{0k}|/n_{2k}$ (see Fig. 2 for $n_{0k} = -0.02$). As a result, the entire dependence $I_{\text{out}}(I_{\text{in}})$ exhibits the typical S-shaped profile inherent to

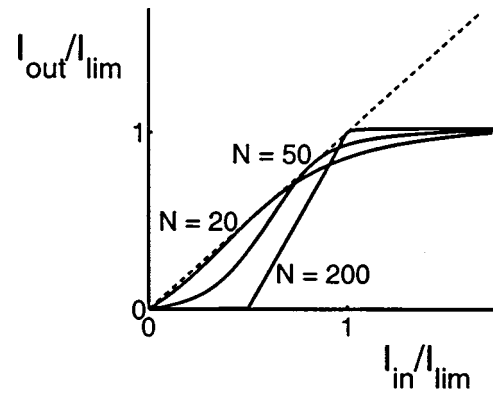


Fig. 3. Balanced nonlinearity management with an out-of-phase grating, where $n_{\text{nl}} = 0$, $n_{0k} = -0.02$, and $n_{2k} = 1$. The figure emphasizes the sharpening of the S-shaped curves with an increase in the number of layers. Each curve has been normalized to its limiting intensity.

bistable transmission regimes.²² Still, the transmitted intensity I_{out} is a one-to-one function of I_{in} and is bounded by its limiting value I_{lim} that satisfies the estimate (21). Thus bistability is not supported in the limit $n_{\text{nl}} = 0$ but, as we show in Subsection 3.B, it can be achieved for the nonlinear out-of-phase periodic structure with unbalanced (nonzero average) nonlinearity management.

The S-shaped input–output transmission characteristics for the out-of-phase gratings enable us to construct a uniform switching device if the structure is sufficiently long, i.e., $N \rightarrow \infty$. Indeed, we show in Fig. 3 for $n_{2k} = 1$ and $n_{0k} = -0.02$ that the transmission curve $I_{\text{out}}(I_{\text{in}})$ becomes a simple two-step map between the lower-transmissive ($I_{\text{out}} = 0$) and higher-transmissive limiting state ($I_{\text{out}} = I_{\text{lim}} = |n_{0k}|/n_{2k}$). By studying the asymptotic behavior of Eq. (22) in the limit $\phi \rightarrow \infty$ ($N \rightarrow \infty$), we derive the following asymptotic formula for intermediate intensities I_{out} ,

$$\frac{I_{\text{out}}}{I_{\text{lim}}} = 2 \frac{I_{\text{in}}}{I_{\text{lim}}} - 1 \quad \text{for } \frac{1}{2}I_{\text{lim}} \leq I_{\text{in}} \leq I_{\text{lim}}. \quad (26)$$

Thus switching between the two states occurs when I_{in} exceeds a threshold given by the $0.5I_{\text{lim}}$ value (see Fig. 3). This two-step map is supported by the out-of-phase gratings only, i.e., when $n_{0k} < 0$. For in-phase gratings, when $n_{0k} \geq 0$, the limit $N \rightarrow \infty$ gives a trivial result,

$$I_{\text{out}} = I_{\text{lim}} = \frac{n_{0k}}{n_{2k}} \quad \text{for } I_{\text{in}} > 0.$$

Provided that the true all-optical limiting is stable for $n_{\text{nl}} = 0$ as shown in Section 4, these results imply that the out-of-phase gratings have sharp features useful in carrying out functions such as limiting, switching, and logic. For instance, the out-of-phase grating with $N = 20$ is suitable for optical limiting, and that for $N = 200$ can be used for logic operations (see Fig. 3).

B. Unbalanced (Nonzero-Average) Nonlinearity

Management: $n_{\text{nl}} \neq 0$

When $n_{\text{nl}} \neq 0$, the analysis becomes more involved. We can still use the connecting relation (15) and find the ex-

act condition when the limiting behavior is possible, i.e., when $Q(0) \rightarrow \infty$ for $I_{\text{out}} \rightarrow I_{\text{lim}} < \infty$. Since $|\cos \Psi| \leq 1$, the limiting regime exists when

$$n_{2k} \geq \frac{3|n_{\text{nl}}|}{4}. \quad (27)$$

In the opposite case, i.e., when $n_{2k} < 3|n_{\text{nl}}|/4$, no limiting regime is possible and the system is bistable or multistable.^{18,22} Figure 4 shows the dependence $I_{\text{out}}(I_{\text{in}})$ for $n_{0k} = 0$, $n_{2k} = 1$, and three values of n_{nl} . The value $n_{\text{nl}} = 1$ fits to the domain (27), and therefore the structure displays the limiting regime. On the other hand, the values $n_{\text{nl}} = 1.4$ and $n_{\text{nl}} = 2$ are outside of the domain (27), and the structure displays multistability that shrinks for strongly unbalanced gratings, i.e., when n_{nl} grows.

In order to study the new features of the limiting regime for $n_{\text{nl}} \neq 0$, we use the relations (12) and (15) to close the system for $Q(Z)$:

$$\left(\frac{dQ}{dZ}\right)^2 = Q(I_{\text{out}} + Q)\{4[n_{0k} + n_{2k}(I_{\text{out}} + 2Q)]^2 - 9n_{\text{nl}}^2 Q(I_{\text{out}} + Q)\}. \quad (28)$$

Simple analysis of the right-hand side of Eq. (28) shows that the system is well defined for the limiting solution when $0 \leq Q(Z) \leq \infty$ if

$$I_{\text{lim}} \geq \frac{4|n_{0k}|}{\sqrt{16n_{2k}^2 - 9n_{\text{nl}}^2}} \quad \text{for } n_{0k} < 0. \quad (29)$$

This constraint improves estimate (21) for $n_{\text{nl}} \neq 0$. Although the explicit solutions of Eq. (28) are given in terms of elliptic functions,²² we construct solutions of Eq. (28) numerically and provide the transmission curve $I_{\text{out}}(I_{\text{in}})$ in Fig. 5 for $n_{\text{nl}} = 1$, $n_{2k} = 1$, and four values of n_{0k} . The curve clearly undertakes only one essential modification compared with the case $n_{\text{nl}} = 0$ (cf. Fig. 2).

Within domain (27) for $n_{\text{nl}} \neq 0$, true all-optical limiting, when $I_{\text{out}}(I_{\text{in}})$ is a one-to-one function clamped below I_{lim} , is supported by the in-phase and weakly out-of-phase gratings (see Fig. 5 for $n_{0k} = -0.02, 0, 0.02$). In this uniform regime the distribution of the reflected wave has a fundamental profile, i.e., it satisfies the following properties: $0 \leq Q(Z) < \infty$ and $dQ(Z)/dZ \leq 0$, for any $0 < I_{\text{out}} \leq I_{\text{lim}}$.

For the sufficiently strong out-of-phase gratings, when $n_{0k} < 0$, multistability takes place at low and high intensities below final limiting behavior as $I_{\text{out}} \rightarrow I_{\text{lim}}$ (see Fig. 5 for $n_{0k} = -0.04$). The limiting intensity I_{lim} satisfies the constraint (29). We refer to this case as locally multistable limiting. It is well known²² that, in contrast to true all-optical limiting, the locally multistable regime leads to complicated dynamics and instabilities in nonlinear periodic optical materials.

In order to find the threshold between the true all-optical limiting and locally multistable limiting for strongly out-of-phase gratings, we deduce from Eq. (28) an asymptotic solution for $Q(Z)$ in the limit $n_{0k} + n_{2k}I_{\text{out}} \rightarrow 0$,

$$Q(Z) = \frac{4(n_{0k} + n_{2k}I_{\text{out}})^2}{9n_{\text{nl}}^2 I_{\text{out}}} \sin^2 \left[\frac{3}{2} n_{\text{nl}} I_{\text{out}} (L - Z) \right]. \quad (30)$$

This expression reduces to Eq. (25) for $n_{\text{nl}} = 0$. It follows from this expression that the profile $Q(Z)$ has the same fundamental properties as for the in-phase gratings, if

$$0 > n_{0k} \geq -\frac{\pi n_{2k}}{3|n_{\text{nl}}|L}. \quad (31)$$

Outside of this domain, i.e., for sufficiently strong out-of-phase mismatch between n_{0k} and n_{2k} or for sufficiently long periodic structures, the profile $Q(Z)$ becomes a non-monotonic function: the derivative dQ/dZ has different signs at $0 \leq Z \leq L$. Further in the domain, when $n_{0k} \leq -2\pi n_{2k}/3|n_{\text{nl}}|L$, the profile $Q(Z)$ has one or more nodes at $0 \leq Z \leq L$. This behavior characterizes local multistability of the periodic structure,²² i.e., the appearance of other branches of I_{out} for a given value of the incident intensity I_{in} . Since the asymptotic solution (30) is valid from both sides of the limit $I_{\text{out}} \rightarrow |n_{0k}|/n_{2k}$, two

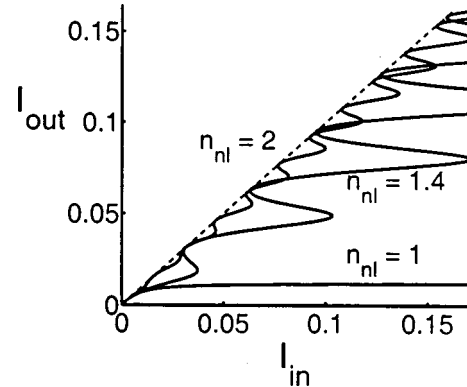


Fig. 4. Unbalanced nonlinearity management with no linear grating, where $n_{0k} = 0$, $n_{2k} = 1$. The threshold between the limiting regime and multistability is $n_{\text{nl}} = 1.33$. Note that the multilevel oscillations become tighter for larger n_{nl} .

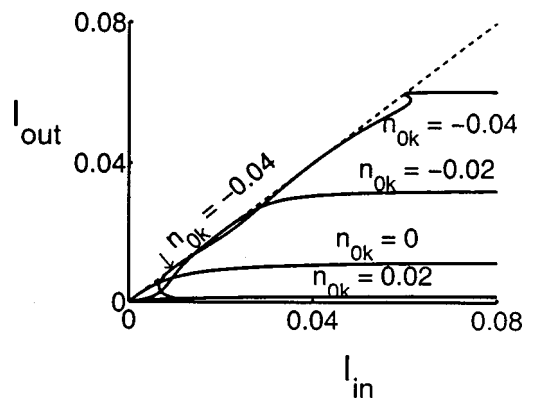


Fig. 5. Unbalanced nonlinearity management with linear grating, where $n_{\text{nl}} = 1$, $n_{2k} = 1$. Bistability occurs for $n_{0k} \leq -0.03$, so the curve for $n_{0k} = -0.04$ shows two local bistability cascades.

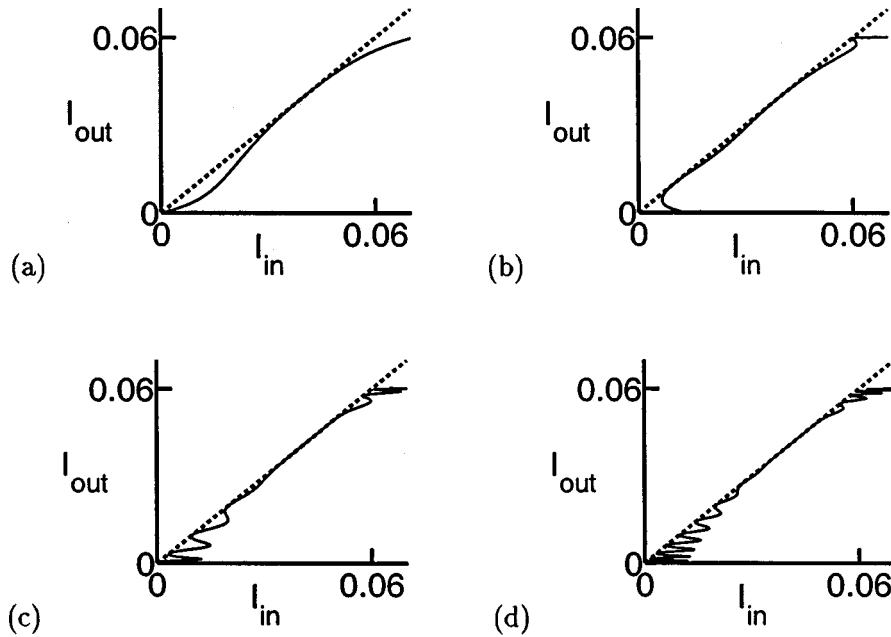


Fig. 6. Unbalanced nonlinearity management with an out-of-phase grating, where $n_{0k} = -0.04$, $n_{nl} = 1$, $n_{2k} = 1$ and (a) $N = 20$, (b) $N = 50$, (c) $N = 200$, and (d) $N = 400$. The I_{out} versus I_{in} curves become multistable as the device gets longer.

casades of local multistability levels must coexist for lower and higher intensities I_{in} (see Fig. 5 for $n_{0k} = -0.04$).

The threshold (31) depends on the size of the structure, i.e., L and N . When the structure becomes longer, a relatively small out-of-phase mismatch n_{0k} leads to multistable behavior and more levels of multistability arise. This is shown in Fig. 6 for $n_{nl} = 1$, $n_{0k} = -0.04$, $n_{2k} = 1$, and different values of N . Thus sharp features of out-of-phase gratings, which could be realized by exact compensating of the Kerr nonlinearity, are destroyed in the out-of-phase structure with nonzero average nonlinearity (cf. Fig. 3 and Fig. 6).

To summarize, we have found that true all-optical limiting exists within the domains (27) and (31), where the limiting intensity I_{out} is estimated for the out-of-phase gratings in Eq. (29). For sufficiently strong or sufficiently long out-of-phase gratings, when constraint (31) is violated, the bistable limiting regime exists within domain (27) with the estimate on I_{lim} given by Eq. (29). Finally, when constraint (27) is violated, i.e., for strongly unbalanced nonlinear gratings, the limiting regime is replaced by the multistable transmission regime.

4. LINEAR STABILITY ANALYSIS

Here we analyze the linear stability of stationary regime of light transmission. Linear stability results characterize time-dependent perturbations that develop in the periodic optical structure over stationary transmission. The stability results determine whether true all-optical limiting does indeed survive under real-life disturbances. If this is the case, then the operating regimes based on true all-optical limiting can be excited experimentally by light incident on the structure.

De Sterke showed²⁵ that periodic nonlinear gratings with no nonlinearity management possess dramatic in-

stabilities for coherent-light transmissions at high intensities. These instabilities are classified into two types. Type I instability occurs for stationary transmission at intermediate intensities where the curve I_{out} versus I_{in} has a negative slope. Type I instability results in switching of the stationary distribution either to lower or to higher transmissive states (with a smaller or larger value of the output intensity I_{out}). The other (type II) instability occurs for high-intensity transmission, i.e., at the upper branch of the bistable curve $I_{out}(I_{in})$. Type II instability is characterized by the nonzero frequencies of the perturbation evolution, which cause the instability to be oscillatory. This instability is manifested through self-pulsations of the periodic structure between high-transmission and low-transmission states.²⁶

We show here for the case $n_{nl} = 0$ that the true all-optical limiting regime exhibits no instabilities of either type I or II and is asymptotically stable. First, we simplify the coupled-mode equations (4) and (5) by linearizing

$$\begin{bmatrix} A_+ \\ \bar{A}_+ \end{bmatrix} (Z, T) = \begin{bmatrix} A_+ \\ \bar{A}_+ \end{bmatrix} (Z) + \begin{bmatrix} a_1 \\ a_2 \end{bmatrix} (Z) \exp(\lambda T), \quad (32)$$

$$\begin{bmatrix} A_- \\ \bar{A}_- \end{bmatrix} (Z, T) = \begin{bmatrix} A_- \\ \bar{A}_- \end{bmatrix} (Z) + \begin{bmatrix} b_1 \\ b_2 \end{bmatrix} (Z) \exp(\lambda T), \quad (33)$$

where the perturbations are considered to be small, i.e., $|a_1|, |a_2|, |b_1|, |b_2| \ll |A_+|, |A_-|$, and λ is the time-evolution constant. The coupled-mode equations (4) and (5) reduce with the help of Eqs. (32) and (33) to the linear eigenvalue problem for the spectrum of λ :

$$\mathbf{H}\psi = \lambda \mathbf{J}\psi, \quad (34)$$

where $\psi = (a_1, b_1, a_2, b_2)^t$ is the perturbation vector, $\mathbf{J} = \text{diag}(i, i, -i, -i)$ is a skew-symmetric operator, and \mathbf{H} is the symmetric Dirac-type operator with the given potential

$$\mathbf{H} = -i \begin{bmatrix} \sigma_3 & 0 \\ 0 & -\sigma_3 \end{bmatrix} \frac{d}{dZ} - n_{0k} \begin{bmatrix} \sigma_1 & 0 \\ 0 & \sigma_1 \end{bmatrix}$$

$$- n_{nl} \begin{bmatrix} 2(|A_+|^2 + |A_-|^2) & 2A_+\bar{A}_- & A_+^2 & 2A_+A_- \\ 2\bar{A}_+A_- & 2(|A_+|^2 + |A_-|^2) & 2A_+A_- & A_-^2 \\ -\bar{A}_+^2 & 2\bar{A}_+\bar{A}_- & 2(|A_+|^2 + |A_-|^2) & 2\bar{A}_+A_- \\ 2\bar{A}_+\bar{A}_- & \bar{A}_-^2 & 2A_+\bar{A}_- & 2(|A_+|^2 + |A_-|^2) \end{bmatrix}$$

$$- n_{2k} \begin{bmatrix} 2(A_+\bar{A}_- + \bar{A}_+A_-) & 2(|A_+|^2 + |A_-|^2) & 2A_+A_- & (A_+^2 + A_-^2) \\ 2(|A_+|^2 + |A_-|^2) & 2(A_+\bar{A}_- + \bar{A}_+A_-) & (A_+^2 + A_-^2) & 2A_+A_- \\ 2\bar{A}_+\bar{A}_- & (\bar{A}_+^2 + \bar{A}_-^2) & 2(A_+\bar{A}_- + \bar{A}_+A_-) & 2(|A_+|^2 + |A_-|^2) \\ (\bar{A}_+^2 + \bar{A}_-^2) & 2\bar{A}_+\bar{A}_- & 2(|A_+|^2 + |A_-|^2) & 2(A_+\bar{A}_- + \bar{A}_+A_-) \end{bmatrix}.$$

Here σ_1 and σ_3 are the Pauli matrices

$$\sigma_1 = \begin{bmatrix} 0 & 1 \\ 1 & 0 \end{bmatrix}, \quad \sigma_3 = \begin{bmatrix} 1 & 0 \\ 0 & -1 \end{bmatrix}.$$

The problem (34) is now well defined: provided that a nonzero perturbation vector $\psi(Z)$ at a certain value of λ does not modify the intensity of the incident wave, the time-evolution constant λ in Eqs. (32) and (33) prescribes the dynamics of internal perturbations in the periodic optical structure. If the internal perturbations can grow with time, i.e., if $\text{Re}(\lambda) > 0$, then the stationary regime is unstable and will be deformed or destroyed by the growing perturbations. Mathematically, the problem is to find solutions of the linear eigenvalue problem (34) that satisfy the following boundary conditions at the left and right ends of the structure,

$$a_1(0) = a_2(0) = b_1(L) = b_2(L) = 0. \quad (35)$$

Such solutions may exist only for special values of λ called eigenvalues of the discrete spectrum. In the case $n_{nl} = 0$ we find exact solutions of Eq. (34) and show that there are no nontrivial eigenvalues for $\text{Re}(\lambda) > 0$. Thus the true all-optical limiting regime is stable for $n_{nl} = 0$.

When $n_{nl} = 0$, the potentials in the operator \mathbf{H} can be expressed through the exact solutions found in Subsection 3.A. Suppose first that $|n_{0k}| \leq n_{2k}I_{\text{out}}$. In this case, $A_+(Z) = -i[I_{\text{out}} + Q(Z)]^{1/2}$ and $A_-(Z) = [Q(Z)]^{1/2}$, where $Q(Z)$ is given by Eq. (18). The linear problem (34) can then be decomposed for two uncoupled vectors,

$$\psi_+(Z) = \begin{bmatrix} a_1 + a_2 \\ b_1 - b_2 \end{bmatrix}(Z), \quad \psi_-(Z) = \begin{bmatrix} a_1 - a_2 \\ b_1 + b_2 \end{bmatrix}(Z). \quad (36)$$

The vectors $\psi_{\pm}(Z)$ satisfy two uncoupled linear problems following from Eq. (34),

$$[\mathbf{H}_1 \pm n_{2k}\mathbf{H}_2]\psi_{\pm} = i\lambda\psi_{\pm}, \quad (37)$$

where \mathbf{H}_1 and \mathbf{H}_2 are respectively symmetric and anti-symmetric operators,

$$\mathbf{H}_1 = -i\sigma_3 \frac{d}{dZ} - \sigma_1[n_{0k} + 2n_{2k}(I_{\text{out}} + 2Q)],$$

$$\mathbf{H}_2 = 2i\sigma_3 \sqrt{Q(I_{\text{out}} + Q)} + \sigma_1\sigma_3 I_{\text{out}}.$$

It follows from Eqs. (18) and (22) that the potential in Eq. (37) has the symmetry $Q(Z) = Q(2L - Z)$. Using this symmetry, we can relate the vectors $\psi_+(Z)$ and $\psi_-(Z)$:

$$\psi_{-1}(Z) = \psi_{+2}(2L - Z), \quad \psi_{-2}(Z) = \psi_{+1}(2L - Z). \quad (38)$$

Thus it is sufficient to study problem (37) for the vector $\psi_+(Z)$ only. We set the variables

$$\theta = \sqrt{n_{2k}^2 I_{\text{out}}^2 - n_{0k}^2}(L - Z), \quad \lambda = \sqrt{n_{2k}^2 I_{\text{out}}^2 - n_{0k}^2}\gamma, \quad (39)$$

where γ is a new time-evolution constant. The vector $\psi_+(Z)$ in problem (37) can be then transformed by the substitution

$$\psi_{+1}(Z) = -i[(n_{2k}I_{\text{out}} - n_{0k})(n_{2k}I_{\text{out}} \cos 2\theta - n_{0k})]^{1/2} \varphi_1(\theta), \quad (40)$$

$$\psi_{+2}(Z) = [(n_{2k}I_{\text{out}} + n_{0k})(n_{2k}I_{\text{out}} \cos 2\theta - n_{0k})]^{1/2} \varphi_2(\theta). \quad (41)$$

As a result, linear problem (37) is rewritten in the final form

$$\frac{d\varphi_1}{d\theta} - \left[1 + \frac{2(n_{0k} + n_{2k}I_{\text{out}})}{n_{2k}I_{\text{out}} \cos 2\theta - n_{0k}} \right] \varphi_2 = \gamma\varphi_1, \quad (42)$$

$$-\frac{d\varphi_2}{d\theta} - \left[1 + \frac{2(n_{0k} - n_{2k}I_{\text{out}})}{n_{2k}I_{\text{out}} \cos 2\theta - n_{0k}} \right] \varphi_1 = \gamma\varphi_2. \quad (43)$$

This linear system is known as the Ablowitz–Kaup–Newell–Segur scheme for integrable evolution equations solvable by inverse scattering.²⁷ The Ablowitz–Kaup–Newell–Segur scheme in the form (42) and (43) includes solutions with nonzero boundary conditions for such equations as the nonlinear Schrödinger and modified Korteweg–de Vries equations. This fact allows us to use substitutions from Ref. 28 and generate exact solutions of the system (42) and (43). There are two solutions for any given value of γ .

$$\begin{aligned} \varphi(\theta) = \Phi_{\pm}(\theta, \gamma) = & \exp(\pm ik\theta) \\ & \times \left[\left(\pm ik + \frac{n_{2k} I_{\text{out}} \sin 2\theta}{n_{2k} I_{\text{out}} \cos 2\theta - n_{0k}} \right) \right. \\ & \times \left(\frac{-(\gamma \pm ik)}{1} \right) + \frac{1}{n_{2k} I_{\text{out}} \cos 2\theta - n_{0k}} \\ & \left. \times \left(\frac{n_{0k} + n_{2k} I_{\text{out}}}{(n_{0k} - n_{2k} I_{\text{out}})(\gamma \pm ik)} \right) \right], \end{aligned} \quad (44)$$

where $k = q\sqrt{1 - \gamma^2}$. The boundary conditions compatible with Eqs. (35) and (36) are read for the vector $\psi_+(Z)$ as

$$\psi_+(Z): \quad \varphi_2(0) = 0, \quad \varphi_1(\theta_0) = 0, \quad (45)$$

where $\theta_0 = \sqrt{n_{2k}^2 I_{\text{out}}^2 - n_{0k}^2} L$. In order to satisfy the boundary conditions (45) we take a linear combination of the two solutions (44), i.e., $\varphi(\theta) = c_1 \Phi_+(\theta, \gamma) + c_2 \Phi_-(\theta, \gamma)$, and reduce the problem to a linear system for c_1 and c_2 . The system has a nonzero solution if γ solves the determinant equation

$$\begin{aligned} D_+(\gamma; u, \theta_0) = & \gamma + \frac{\sin 2\theta_0}{\cos 2\theta_0 - \mu} - \frac{\tan(k\theta_0)}{k} \\ & \times \left(k^2 + \frac{1 + \mu - \gamma \sin 2\theta_0}{\cos 2\theta_0 - \mu} \right) = 0, \end{aligned} \quad (46)$$

where $\mu = n_{0k}/(n_{2k} I_{\text{out}})$, $k = \sqrt{1 - \gamma^2}$, and $\theta_0 = n_{2k} I_{\text{out}} \sqrt{1 - \mu^2}$.

On the other hand, the boundary conditions for the vector $\psi_-(Z)$ can be rewritten with the help of Eqs. (35)–(41) as

$$\psi_-(Z): \quad \varphi_1(0) = 0, \quad \varphi_2(-\theta_0) = 0. \quad (47)$$

Once again, in order to satisfy the boundary conditions (47) we take a linear combination of the two solutions (44), i.e., $\varphi(\theta) = c_1 \Phi_+(\theta, \gamma) + c_2 \Phi_-(\theta, \gamma)$, and reduce the problem to a linear system for c_1 and c_2 . The system has a nonzero solution if γ solves the determinant equation

$$\begin{aligned} D_-(\gamma, \mu, \theta_0) = & 2 - \gamma^2(1 - \mu) - \frac{(2 + \gamma \sin 2\theta_0)(1 - \mu)}{\cos 2\theta_0 - \mu} \\ & + \frac{\tan(k\theta_0)}{k} \left\{ (1 - \mu) \gamma k^2 \right. \\ & \left. + \frac{\gamma(1 - \mu^2) + [2 - \gamma^2(1 - \mu)] \sin 2\theta_0}{\cos 2\theta_0 - \mu} \right\} = 0. \end{aligned} \quad (48)$$

Thus the analysis of the linear problem (37) reduces to finding complex zeros of the functions $D_{\pm}(\gamma)$ given by Eqs. (46) and (48). Figures 7(a)–7(d) show behavior of the functions $D_+(\gamma)$ and $D_-(\gamma)$, respectively, at real values of γ for several values of the parameters $|\mu| \leq 1$ and θ_0 . It is clear from the figures that no zeros of $D_{\pm}(\gamma)$ exist for $\gamma \neq 0$. At $\gamma = 0$ there is a single zero of $D_+(\gamma)$ and a double zero of $D_-(\gamma)$. These solutions for $\gamma = 0$ reproduce in fact trivial (i.e., identically zero) solutions of Eqs. (42) and (43) that can be neglected. Thus we have shown that there are no nontrivial solutions of Eq. (34) for real values of γ .

In a complex domain of γ we analyzed the functions $D_{\pm}(\gamma)$ by using Mathematica. Zeros of $D_{\pm}(\gamma)$ were found only in the domain where $\text{Re}(\gamma) < 0$ and $\text{Im}(\gamma) \neq 0$. Indeed, the functions $D_{\pm}(\gamma)$ are exponentially growing for $\text{Re}(\lambda) > 0$ (see Fig. 7) and cannot have zeros in this domain of the complex plane. Also one can show from Eqs.

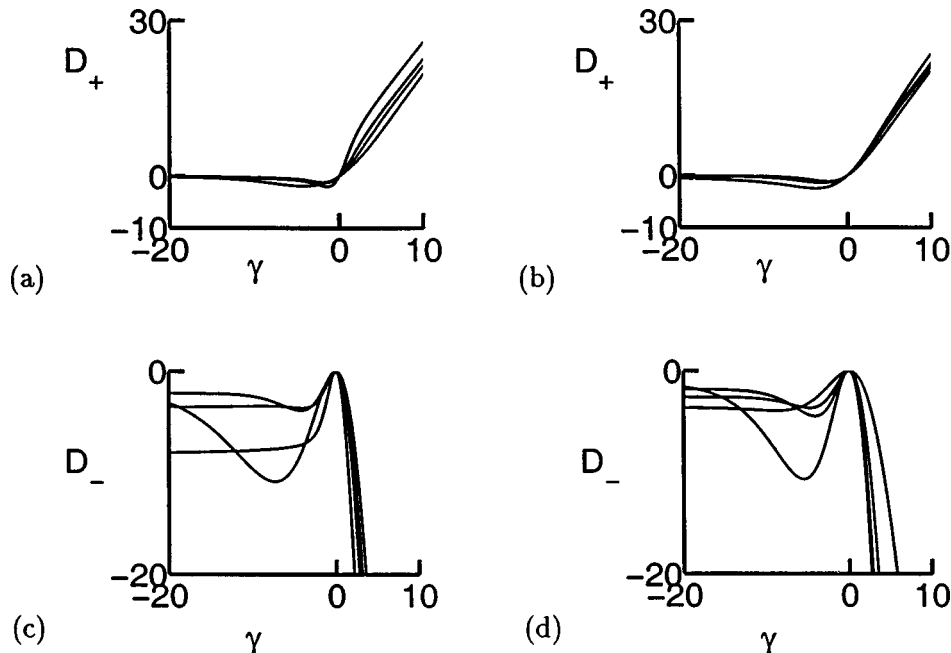


Fig. 7. (a), (b) Functions D_+ and (c), (d) D_- versus γ as given in Eqs. (46) and (48) for two sets: (a), (c) $\mu = 0$ and $\theta_0 = 0.25\pi$ [0.2, 0.4, 0.6, 0.8]; (b), (d) $\mu = -0.75, -0.25, 0.25, 0.75$, and $\theta_0 = 0.1\pi(1 - \mu^2)^{1/2}$. No zeros of $D_{\pm}(\gamma)$ exist for $\gamma \neq 0$.

(46) and (48) that zeros of $D_{\pm}(\gamma)$ cannot exist for $\text{Re}(\lambda) = 0$ and $\text{Im}(\lambda) \neq 0$. Thus the domain for zeros of $D_{\pm}(\gamma)$ is constrained by the left half-plane: $\text{Re}(\lambda) < 0$ and $\text{Im}(\gamma) \neq 0$. These describe oscillatory and exponentially decaying perturbations that gradually vanish in time dynamics of the periodic nonlinear structure.

Thus we summarize that the highly transmissive state in the true all-optical limiting regime is asymptotically stable, i.e., small perturbations of stationary regimes are decaying exponentially. The stability results are valid for exact compensation of the Kerr nonlinearity in the structure, i.e., for $n_{\text{nl}} = 0$. Both type I and type II instabilities discovered for linear gratings with no compensation of the Kerr nonlinearities²⁵ do not show up for true all-optical limiting.

The previous analysis was performed for $|n_{0k}| \leq n_{2k}I_{\text{out}}$, i.e., for $|\mu| \leq 1$. In the opposite case, when $|n_{0k}| > n_{2k}I_{\text{out}}$, i.e., $|\mu| > 1$, the potential $Q(Z)$ in the linear problem (37) is expressed by Eq. (22). Since the connection between Eqs. (18) and (22) is $\theta = i\phi$, we extend the determinant equations (46) and (48) by replacing $\theta_0 = i\phi_0$ and $\gamma = -i\Gamma$ [the latter condition ensures λ in Eqs. (32), (33), and (39) is proportional to Γ]. Then, the spectrum of the linear problem (37) is given by zeros of the modified functions $D_{\pm}(\gamma)$:

$$\begin{aligned} \hat{D}_+(\Gamma; \mu, \phi_0) &= \Gamma + \frac{\sinh 2\phi_0}{\mu - \cosh 2\phi_0} + \frac{\tanh(\kappa\phi_0)}{\kappa} \\ &\times \left(\kappa^2 - \frac{1 + \mu - \Gamma \sinh 2\phi_0}{\mu - \cosh 2\phi_0} \right) = 0, \end{aligned} \quad (49)$$

$$\begin{aligned} \hat{D}_-(\Gamma, \mu, \phi_0) &= 2 + \Gamma^2(1 - \mu) + \frac{(2 + \Gamma \sinh 2\phi_0)(1 - \mu)}{\mu - \cosh 2\phi_0} \\ &+ \frac{\tanh(\kappa\phi_0)}{\kappa} \left\{ (1 - \mu)\Gamma\kappa^2 \right. \\ &\left. - \frac{\Gamma(1 - \mu^2) - [2 + \Gamma^2(1 - \mu)]\sinh 2\phi_0}{\mu - \cosh 2\phi_0} \right\} = 0, \end{aligned} \quad (50)$$

where $\mu = n_{0k}/(n_{2k}I_{\text{out}})$, $\kappa = \sqrt{1 + \Gamma^2}$, and $\phi_0 = n_{2k}I_{\text{out}}L\sqrt{\mu^2 - 1}$. The functions $\hat{D}_{\pm}(\Gamma)$ for $|\mu| > 1$ are not shown but appear similar to Fig. 7. The only new feature is that these functions have an additional single zero for real negative values of Γ . This additional zero corresponds to exponentially decaying stable perturbations of the nonlinear structure. Any zeros for real and complex values of Γ with $\text{Re}(\Gamma) > 0$ are absent. Thus we conclude again that true all-optical limiting is asymptotically stable for the whole range of I_{in} and I_{out} in the balanced nonlinear grating, when $n_{\text{nl}} = 0$.

5. CONCLUSION

We summarize that true all-optical limiting is best achieved when the Kerr nonlinearity is compensated *exactly* across the alternating layers, i.e., when the net-

average nonlinearity is zero. In this case a small addition of the out-of-phase linear grating transforms the periodic nonlinear structure to an ideal uniform switch with an abrupt transfer characteristic. Such stable devices are useful in needed optical signal grooming functions such as optical limiting, logic, and signal processing. There are three factors that affect performance of such uniform switches: mismatch between the linear and nonlinear refractive indices, the length of the structure, and net-average nonlinearity. Local multistability destroys the uniform limiting features when the mismatch is sufficiently large or the structure is sufficiently long and the net-average nonlinearity is nonzero. Although the in-phase gratings do not display a two-step uniform map, they are more robust with respect to any of these three factors to serve as stable limiters. In paper II we will report numerical simulations of the coupled model and confirm asymptotic stability of true all-optical limiting in nonstationary dynamics of the periodic structure.

ACKNOWLEDGMENTS

The authors thank G. Darling and E. Johnson for useful collaborations and remarks on improving the manuscript.

REFERENCES

1. P. W. E. Smith and L. Qian, "Switching to optical for a faster tomorrow," *IEEE Circuits Devices Mag.* **15**(11), 28–33 (1999).
2. N. S. Patel, K. L. Hall, and K. A. Rauschenbach, "Interferometric all-optical switches for ultrafast signal processing," *Appl. Opt.* **37**, 2831–2842 (1998).
3. P. Tran, "All-optical switching with a nonlinear chiral photonic bandgap structure," *J. Opt. Soc. Am. B* **16**, 70–73 (1999).
4. G. L. Wood, W. W. Clark III, M. J. Miller, G. J. Salamo, and E. J. Sharp, "Evaluation of passive optical limiters and switches," *Proc. SPIE* **1105**, 154–166 (1989).
5. T. Xia, D. J. Hagan, A. Dogariu, A. A. Said, and E. W. Van Stryland, "Optimization of optical limiting devices based on excited-state absorption," *Appl. Opt.* **36**, 4110–4122 (1997).
6. I. C. Khoo, M. Wood, B. D. Guenther, "Nonlinear liquid crystal fiber array for all-optical switching/limiting," in *Proceedings of the Ninth Annual Meeting of the IEEE Lasers and Electro-Optics Society* (IEEE, New York, 1996), Vol. 2, pp. 211–212.
7. F. E. Hernandez, S. Yang, E. W. Van Stryland, and D. J. Hagan, "High-dynamic-range cascaded-focus optical limiter," *Opt. Lett.* **25**, 1180–1182 (2000).
8. M. W. Chbat, B. Hong, M. N. Islam, C. E. Socolich, and P. R. Prucnal, "Ultrafast soliton-trapping AND gate," *J. Lightwave Technol.* **10**, 2011–2016 (1992).
9. M. N. Islam, C. E. Socolich, C.-J. Chen, K. S. Kim, J. R. Simpson, and U. C. Paek, "All-optical inverter with one picosecond switching energy," *Electron. Lett.* **27**, 130–132 (1991).
10. A. Niiyama and M. Koshihara, "Three-dimensional beam propagation analysis of nonlinear optical fibers and optical logic gates," *J. Lightwave Technol.* **16**, 162–168 (1998).
11. L. Brzozowski and E. H. Sargent, "Optical signal processing using nonlinear distributed feedback structures," *IEEE J. Quantum Electron.* **36**, 550–555 (2000).
12. H. G. Winful, J. H. Marburger, and E. Garmire, "Theory of bistability in nonlinear distributed feedback structure," *Appl. Phys. Lett.* **35**, 379–381 (1979).
13. P. W. Smith, "Bistable optical devices promise subpicosecond switching," *IEEE Spectrum* **8**(6), 26–30 (1981).
14. C.-X. Shi, "Optical bistability in reflective fiber grating," *IEEE J. Quantum Electron.* **31**, 2037–2043 (1995).
15. S. Dubovitsky and W. H. Steier, "Analysis of optical bista-

- bility in a nonlinear coupled resonator," *IEEE J. Quantum Electron.* **28**, 585–589 (1992).
16. J. He and M. Cada, "Optical bistability in semiconductor periodic structures," *IEEE J. Quantum Electron.* **27**, 1182–1188 (1991).
 17. H. G. Winful and G. D. Cooperman, "Self-pulsing and chaos in distributed feedback bistable optical devices," *Appl. Phys. Lett.* **40**, 298–300 (1982).
 18. D. E. Pelinovsky, L. Brzozowski, and E. H. Sargent, "Transmission regimes of periodic nonlinear optical structures," *Phys. Rev. E* **62**, R4536–R4539 (2000).
 19. M. M. Fejer, G. A. Magel, D. H. Jundt, and R. L. Byer, "Quasi-phase-matched second harmonic generation: tuning and tolerances," *IEEE J. Quantum Electron.* **28**, 2631–2654 (1992).
 20. A. Kobayakov, F. Lederer, O. Bang, and Yu. S. Kivshar, "Nonlinear phase shift and all-optical switching in quasi-phase-matching quadratic media," *Opt. Lett.* **23**, 506–508 (1998).
 21. S. Trillo, C. Conti, G. Assanto, and A. V. Buryak, "From parametric gap solitons to chaos by means of second-harmonic generation in Bragg gratings," *Chaos* **10**, 590–599 (2000).
 22. C. M. de Sterke and J. E. Sipe, "Gap solitons," *Prog. Opt.* **33**, 203–260 (1994).
 23. B. E. A. Saleh and M. C. Teich, *Fundamentals of Photonics* (Wiley, New York, 1991).
 24. E. Kumacheva, O. Kalinina, and L. Lige, "Three-dimensional arrays in polymer nanocomposites," *Adv. Mater.* **11**, 231–234 (1999).
 25. C. M. de Sterke, "Stability analysis of nonlinear periodic media," *Phys. Rev. A* **45**, 8252–8258 (1992).
 26. C. M. de Sterke and J. E. Sipe, "Switching dynamics of finite periodic nonlinear media: a numerical study," *Phys. Rev. A* **42**, 2858–2869 (1990).
 27. M. J. Ablowitz, D. J. Kaup, A. C. Newell, and H. Segur, "The inverse scattering transform—Fourier analysis for nonlinear problems," *Stud. Appl. Math.* **53**, 249–315 (1974).
 28. D. E. Pelinovsky and R. H. J. Grimshaw, "Structural transformation of eigenvalues for a perturbed algebraic soliton potential," *Phys. Lett. A* **229**, 165–172 (1997).